Thermalization process in a one-dimensional lattice with two-dimensional motions: The role of angular momentum conservation

Yanjiang Guo (郭彦江), Yachao Sun (孙亚超), and Lei Wang (王雷)*
Department of Physics, Beijing Key Laboratory of Opto-electronic Functional Materials and Micro-nano Devices, and Key Laboratory of Quantum State Construction and Manipulation (Ministry of Education), Renmin University of China, Beijing 100872, People's Republic of China

(Received 17 April 2023; revised 5 June 2023; accepted 27 June 2023; published 25 July 2023)

We study the thermalization process in a one-dimensional lattice with two-dimensional motions. The phonon modes in such a lattice consist of two branches. Unlike in general nonlinear Hamiltonian systems, for which the only conserved quantity is the total energy, the total angular momentum J is also conserved in this system. Consequently, the intra- and interbranch energy transports behave significantly differently. For the intrabranch transport, all the existing rules for the one-dimensional systems including the Chirikov overlap criterion apply. As for the interbranch transport, some trivial processes in one-dimensional lattices become nontrivial. During these processes, all the conservation laws can be satisfied exactly; thus the Chirikov criterion does not apply. These processes provide some fast channels for the interbranch transport, although the thermalization cannot be reached through them alone. A system with nonzero-J initial state, however, can never be thermalized to an equipartition state having zero J. Quite counterintuitively, the corresponding asymptotic mode energy distribution greatly concentrates to a few lowest-frequency modes in one branch.

DOI: 10.1103/PhysRevE.108.014127

I. INTRODUCTION

An N-degree-of-freedom time-independent Hamiltonian system is said to be integrable if there exist N independent conserved quantities. The trajectory of such an integrable system in the phase space is restricted to lie on an N-dimensional torus. Commonly nonlinearity breaks most of the conservations; thus a nonlinear Hamiltonian system is generally nonintegrable due to insufficient number of conserved quantities [1]. A very special exception is the Toda lattice [2], which is nonlinear but integrable. For general nonintegrable systems, e.g., the famous the Fermi-Pasta-Ulam (FPU) lattice [3], the only remaining conserved quantity is the total energy. In a high-degree-of-freedom ($N \geqslant 3$) case, since any small nonlinear perturbation breaks all the rational Kolmogorov-Arnold-Moser (KAM) tori and the remaining ones are not able to divide the energy surface, it is commonly assumed that a trajectory from any initial state (except for some with zero measurement) will eventually be able to visit the whole energy surface uniformly; i.e., the system reaches an equipartition state.

On the other hand, despite the above clear picture, the detailed thermalization process might be very complicated and last an extremely long time. The thermalization time may depend on the magnitude of nonlinearity very sensitively, in particular in the weakly nonlinear cases. A pioneering study showed that the equipartition cannot be observed in weakly nonlinear FPU lattices in an affordable timescale, known as the FPU paradox [3]. This major step has led to the discovery of solitons in nonlinear physics [4]. Very recently, it was revealed that the scaling exponent of the Lyapunov time is the same as the thermalization time, which illustrates explicitly how the thermalization process is related quantitatively to the intrinsic chaotic property [5].

The energy carriers of various lattice models can be characterized by phonons [6], which were proposed originally to describe the noninteracting harmonic normal modes in linear systems. In weakly nonlinear systems, renormalization phonons which slightly interact with each other are proposed instead [7–15]. The wave turbulence theory was then proposed [16–21]. It suggests that in a weakly nonlinear system, the thermalization process is governed by the nontrivial multiwave resonances, e.g., the umklapp phonon scattering process. Such a theory has been widely applied to FPU-type lattices [22–29], the perturbed Toda lattice [30], the discrete nonlinear Klein-Gordon chain [31], waves in the ocean [32], and also heat conduction in particle lattices [33]. In such a scenario, for a lattice with finite size and thus with discrete phonon modes, the so-called Chirikov overlap criterion [34] applies; i.e., the harmonic modes are broadened by the nonlinearity and when the broadening is greater than the frequency spacing, i.e., the frequency distance between two adjacent modes, the conditions for the resonances may be satisfied and thus the thermalization is fast.

In this paper, we study the thermalization process in a one-dimensional lattice, in which the motion of each particle is in two transverse dimensions. In contrast to a general nonlinear Hamiltonian system, in which the only conserved quantity is the total energy, the total angular momentum J is also conserved. This extra conservation changes the dynamics of the system largely and thus provides a lot of new physical

*phywanglei@ruc.edu.cn

 ©2023 American Physical Society

pictures. The rest of the paper is organized as follows. The model is introduced in Sec. II. In Sec. III, the normalized phonon modes in such a lattice and then the quantitative measure of equipartition are introduced. In Sec. IV we show that due to the total angular momentum conservation, a system with nonzero J can never reach an equipartition state. An asymptotic state in such a case will be analytically worked out. The quite different approaches of intra- and interbranch energy transports are presented in Sec. V. The thermalization process from zero angular momentum initial conditions thus ends at an equipartition state, which is studied in Sec. VI. The nonlinearity-induced mode frequency shift and broadening will be calculated. Finally, a summary and discussion are provided in Sec. VII.

II. MODEL

The model we study is a one-dimensional (1D) lattice with two-dimensional (2D) motions, whose Hamiltonian reads

$$H = \sum_{j=1}^{N} \frac{1}{2}|\vec{p}_j|^2 + V(|\vec{q}_{j+1} - \vec{q}_j|), \tag{1}$$

where N denotes the total number of particles and all the masses have been set to unity. $\vec{q}_j \equiv x_j\vec{e}_x + y_j\vec{e}_y$ and $\vec{p}_j \equiv v_{xj}\vec{e}_x + v_{yj}\vec{e}_y$. Hereafter, we call it a quasi-2D lattice. Fixed boundary conditions are applied, i.e., $x_0 = y_0 = x_{N+1} = y_{N+1} = 0$. The interaction potential V takes a FPU-β type,

$$V(r) = \frac{K}{2}r^2 + \frac{\lambda}{4}r^4. \tag{2}$$

Then Hamiltonian (1) can be written as

$$H = \sum_{j=1}^{N}\left[\frac{1}{2}\left(v_{xj}^2 + v_{yj}^2\right) + \frac{K}{2}\left(\Delta x_j^2 + \Delta y_j^2\right) + \frac{\lambda}{4}\left(\Delta x_j^4 + 2\Delta x_j^2\Delta y_j^2 + \Delta y_j^4\right)\right], \tag{3}$$

where $\Delta x_j \equiv x_{j+1} - x_j$ and $\Delta y_j \equiv y_{j+1} - y_j$. Unless otherwise stated, K and λ are always fixed to unity throughout this paper.

The total angular momentum

$$J \equiv \sum_{j=1}^{N}(v_{xj}y_j - v_{yj}x_j). \tag{4}$$

It is easily confirmed that its Poisson bracket with H,

$$\{J, H\} \equiv \sum_{j=1}^{N}\left[\frac{\partial J}{\partial x_j}\frac{\partial H}{\partial v_{xj}} - \frac{\partial J}{\partial v_{xj}}\frac{\partial H}{\partial x_j} + \frac{\partial J}{\partial y_j}\frac{\partial H}{\partial v_{yj}} - \frac{\partial J}{\partial v_{yj}}\frac{\partial H}{\partial y_j}\right], \tag{5}$$

equals zero for any kind of $V(r)$, harmonic or anharmonic; thus J is always conserved. Unlike the momentum conservation, this conservation will not be broken by the fixed boundaries. We will see that this extra conserved quantity plays a very important role in the dynamics of this system. If the cross term $2\Delta x_j^2\Delta y_j^2$ in Eq. (3) is omitted, the system reduces to two independent 1D lattices [35] and this conservation is broken. In some previous studies, stochastic momentum exchanges are applied [36], which will also break this conservation.

III. NORMALIZED MODES AND MEASURE OF EQUIPARTITION

A. Harmonic phonon modes

The dynamics that corresponds to the linearized Hamiltonian follows

$$dv_{xj} = (\Delta x_j - \Delta x_{j-1})dt, \tag{6}$$

$$dv_{yj} = (\Delta y_j - \Delta y_{j-1})dt. \tag{7}$$

The elements of the harmonic matrix reads $\Phi_{jk} = \frac{\partial^2 H}{\partial\rho_j\partial\rho_k}$, where ρ denotes any one of x or y. The matrix takes the form

$$\mathbf{\Phi} \equiv \begin{pmatrix} \mathbf{\Phi}_{1D} & 0 \\ 0 & \mathbf{\Phi}_{1D} \end{pmatrix}, \tag{8}$$

where $\mathbf{\Phi}_{1D}$ is the harmonic matrix of the corresponding 1D linear lattice. For the fixed boundary conditions that we applied, it is a tridiagonal matrix with the nonzero elements $\Phi_{1Djj} = 2$ and $\Phi_{1Dj,j-1} = \Phi_{1Dj-1,j} = -1$.

$\mathbf{\Phi}_{1D}$ can be diagonalized by a unitary transformation matrix $\mathbf{U}$, i.e.,

$$\mathbf{U}^\dagger\mathbf{\Phi}_{1D}\mathbf{U} = \mathbf{\Omega}^2. \tag{9}$$

Each column of $\mathbf{U}$ represents a normal mode $\vec{u}_k$ of the 1D lattice and $\mathbf{\Omega}$ is a diagonal matrix with the nonzero elements $\Omega_{kk} = \omega_k$, where

$$u_{jk} = \sqrt{\frac{2}{N+1}}\sin\frac{jk\pi}{N+1}, \tag{10}$$

$$\omega_k = 2\sin\frac{k\pi}{2(N+1)}. \tag{11}$$

For the quasi-2D lattice, there are $2N$ normal modes. We choose

$$P_{k\pm} = P_{Yk} \mp \omega_k Q_{Xk}, \tag{12}$$

$$Q_{k\pm} = P_{Xk} \pm \omega_k Q_{Yk}, \tag{13}$$

where

$$P_{Xk} = \sum_{j=1}^{N} v_{xj}u_{jk},\ P_{Yk} = \sum_{j=1}^{N} v_{yj}u_{jk}, \tag{14}$$

$$Q_{Xk} = \sum_{j=1}^{N} x_j u_{jk},\ Q_{Yk} = \sum_{j=1}^{N} y_j u_{jk}. \tag{15}$$

The canonical equations are satisfied for the new canonical variables $Q_{k\pm}$ and $P_{k\pm}$, and the linearized Hamiltonian can be written as

$$H = \sum_{k=1}^{N}(E_{k+} + E_{k-}) = \sum_{k=1}^{N}(\omega_{k+}|a_{k+}|^2 + \omega_{k-}|a_{k-}|^2), \tag{16}$$

where the complex normal variables read

$$a_{k\pm} = \frac{iP_{k\pm} \pm Q_{k\pm}}{2\sqrt{\omega_{k\pm}}}. \tag{17}$$

Apparently, $\omega_{k+} = \omega_{k-} = \omega_k$. The normal modes are then divided into two branches, a positive branch and a negative branch. Hereafter, we call a phonon in the positive or negative branch a positive phonon (PP) or a negative phonon (NP), respectively.

Based on the reversed transforms of Eqs. (12)–(15), the total angular momentum J can be written as

$$\begin{aligned} J &= \sum_{j=1}^{N}\sum_{k=1}^{N}\sum_{k'=1}^{N}(P_{Xk}Q_{Yk'} - P_{Yk'}Q_{Xk})u_{jk}u_{jk'} \\ &= \sum_{k=1}^{N}\sum_{k'=1}^{N}(P_{Xk}Q_{Yk'} - P_{Yk'}Q_{Xk})\delta_{kk'} \\ &= \sum_{k=1}^{N}(|a_{k+}|^2 - |a_{k-}|^2) = \sum_{k=1}^{N}(J_{k+} + J_{k-}), \end{aligned} \tag{18}$$

where $\delta_{kk'}$ denotes the Kronecker delta function and

$$J_{k\pm} \equiv \pm|a_{k\pm}|^2 = \pm\frac{E_{k\pm}}{\omega_k} \tag{19}$$

denotes the angular momentum in each mode. It is quite interesting that a PP (NP) always takes one unit of positive (negative) angular momentum, regardless of its wave vector k. A direct consequence is that in any possible phonon scattering, the net number of PPs, i.e., the number of PPs minus the number of NPs, must be conserved.

It is worth mentioning that, due to the degeneracy of the system, the choice of the normal modes $P_{k\pm}$, $Q_{k\pm}$, and consequently the normal variables $a_{k\pm}$, may vary. Our choice, Eqs. (12) and (13), guarantees that the total angular momentum can be written as the summation of the angular momentum in each mode. This provides not only clear physical pictures but great convenience for later analyses as well. Furthermore, Eqs. (18) and (19) are always exact, no matter whether the interaction potential $V(r)$ is harmonic or anharmonic, although in the latter case the total mode energy is no longer conserved.

B. Mode energy distribution and spectral entropy

To quantitatively measure the degree of equipartition, a normalized quantity ξ is defined as [37–39]

$$\xi(t) \equiv e^{\frac{S(t)}{2N}}, \tag{20}$$

where the rescaled spectral entropy

$$S(t) \equiv -\sum_{k=1}^{N}[f_{k+}(t)\ln f_{k+}(t) + f_{k-}(t)\ln f_{k-}(t)], \tag{21}$$

and the rescaled mode energy distribution

$$f_{k\pm}(t) \equiv \frac{2NE_{k\pm}(t)}{\sum_{k=1}^{N}[E_{k+}(t) + E_{k-}(t)]}. \tag{22}$$

In the equipartition states, such defined $f_{k\pm} = 1$, $\forall k$ and ξ approaches its maximum value of 1. The equipartition time $t_{\rm eq}$ is defined as the time when $\xi(t_{\rm eq}) = \frac{1}{2}$.

In the following, thermalization processes from various initial states, with nonzero and zero J, will be studied.

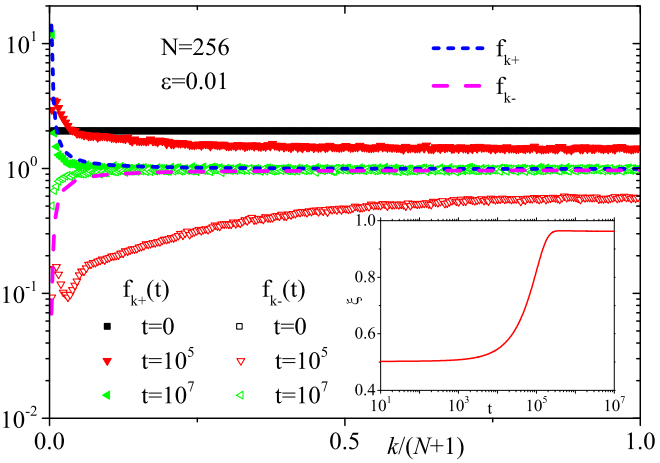

FIG. 1. The rescaled mode energy distribution $f_{k\pm}(t)$ for various times t. The energy is initially put into the positive branch uniformly. The average mode energy $\varepsilon = 0.01$. $N = 256$. Each average is taken over about 4500 independent realizations. The two curves denote the analytically expected asymptotic distributions $f_{k\pm}$, which are described in Eq. (27). Inset: The normalized quantity ξ versus time t. It approaches asymptotically the value determined by Eqs. (37) and (38). It can never reach the equipartition value of 1.

IV. ASYMPTOTIC MODE ENERGY DISTRIBUTION FOR SYSTEMS WITH NONZERO TOTAL ANGULAR MOMENTUM

We have shown in Eq. (5) that, in contrast to many widely studied nonlinear Hamiltonian systems, for which the only conserved quantity is the total energy, the total angular momentum J is also conserved in this system. Due to the symmetry, J in the equilibrium state with equipartition must be zero. Therefore, such an equilibrium state can never be reached from those initial states with nonzero J. Here we emphasize that one is able to remove the nonzero total momentum of a momentum-conserving system by taking a center-of-mass coordinate. The similar operation, however, does not apply to remove the nonzero angular momentum, because, unlike the total mass, the total rotary inertia of this system is not a constant.

To study the thermalization process from those nonzero-J states, we put the energy initially into the positive branch uniformly, i.e., $f_{k+}(0) = 2$ and $f_{k-}(0) = 0$, $\forall k$. Since the angular momentum in each mode in this branch is positive, the total angular momentum J must be largely positive. The rescaled mode energy distributions for various times t are plotted in Fig. 1. An energy concentration to a few low-frequency modes in the positive branch can be clearly observed. Such an energy concentration can be easily understood. Intuitively speaking, compared with the flat initial distribution, some energy moved to the negative branch. This part of the energy contributes negative angular momentum. Therefore, in order to hold the total angular momentum conservation, the positive branch has to contribute more positive angular momentum with, however, less energy. As a result, the energy has to concentrate to the low-frequency modes, because according to Eq. (19), the lower the frequency the more efficiently angular momentum is created.

To quantitatively determine the detailed asymptotic distribution, suppose that such a distribution still maximizes the rescaled spectral entropy S, however, under the conditions of not only the energy conservation,

$$g_1 \equiv \sum_{k=1}^{N}(f_{k+} + f_{k-}) - 2N = 0, \tag{23}$$

but also the angular momentum conservation,

$$g_2 \equiv \sum_{k=1}^{N} \frac{f_{k+} - f_{k-}}{\omega_k} - 2NA = 0, \tag{24}$$

where $A \equiv \frac{J}{E}$ denotes the rescaled total angular momentum.

To find such a distribution, let the Lagrange function be

$$G = S + \mu_1 g_1 + \mu_2 g_2, \tag{25}$$

where μ_1 and μ_2 denote the two Lagrange multipliers. The following partial differential equations are satisfied when G reaches its extremum:

$$\frac{\partial G}{\partial f_{k\pm}} = -\ln f_{k\pm} - 1 + \mu_1 \pm \frac{\mu_2}{\omega_k} = 0. \tag{26}$$

The solution reads

$$f_{k\pm} = e^{-1+\mu_1 \pm \frac{\mu_2}{\omega_k}}, \tag{27}$$

and consequently the two Lagrange multipliers can be determined by solving the following equation group:

$$\sum_{k=1}^{N}(e^{-1+\mu_1+\frac{\mu_2}{\omega_k}} + e^{-1+\mu_1-\frac{\mu_2}{\omega_k}}) = 2N, \tag{28}$$

$$\sum_{k=1}^{N} \frac{e^{-1+\mu_1+\frac{\mu_2}{\omega_k}} - e^{-1+\mu_1-\frac{\mu_2}{\omega_k}}}{\omega_k} = 2NA. \tag{29}$$

For small enough A, applying the first-order approximation, i.e., $e^x \sim 1 + x$, to Eqs. (28) and (29) yields

$$\sum_{k=1}^{N}\left(\mu_1 + \frac{\mu_2}{\omega_k} + \mu_1 - \frac{\mu_2}{\omega_k}\right) = 2N\mu_1 = 2N, \tag{30}$$

$$\sum_{k=1}^{N} \frac{\mu_1 + \frac{\mu_2}{\omega_k} - \mu_1 + \frac{\mu_2}{\omega_k}}{\omega_k} = 2\mu_2 \sum_{k=1}^{N} \frac{1}{\omega_k^2} = 2NA. \tag{31}$$

Thus the first-order approximations of μ_1 and μ_2 read

$$\mu_1 = 1, \tag{32}$$

$$\mu_2 = \frac{NA}{\sum_{k=1}^{N} \frac{1}{\omega_k^2}} \xrightarrow{N\to\infty} \frac{6A}{(N+1)}. \tag{33}$$

Substituting the value of μ_2 into Eq. (28) and taking the second-order approximation $e^x \sim 1 + x + \frac{1}{2}x^2$, we have

$$\sum_{k=1}^{N} e^{-1+\mu_1+\frac{\mu_2}{\omega_k}} + e^{-1+\mu_1-\frac{\mu_2}{\omega_k}} \sim e^{-1+\mu_1} \sum_{k=1}^{N}\left(2 + \frac{\mu_2^2}{\omega_k^2}\right)$$

$$\sim \mu_1(2N + 6A^2) = 2N. \tag{34}$$

Therefore, the second-order approximation of μ_1 reads

$$\mu_1 \sim 1 - \frac{3A^2}{N}. \tag{35}$$

Finally, we have

$$f_{k\pm} = e^{-\frac{3A^2}{N} \pm \frac{6A}{(N+1)\omega_k}}, \tag{36}$$

and the rescaled spectral entropy

$$S = -\sum_{k=1}^{N}\left[\left(-1 + \mu_1 + \frac{\mu_2}{\omega_k}\right)e^{-1+\mu_1+\frac{\mu_2}{\omega_k}} + \left(-1 + \mu_1 - \frac{\mu_2}{\omega_k}\right)e^{-1+\mu_1-\frac{\mu_2}{\omega_k}}\right]$$

$$= 2N(1 - \mu_1 - A\mu_2) = -6A^2 \leqslant 0. \tag{37}$$

In the special case that $A = 0$, $f_{k\pm} = 1$, $\forall k$, and $S = 0$. The equipartition is recovered.

Under the above-mentioned one-branch initial condition, the rescaled total angular momentum is

$$A = \frac{1}{2N}\sum_{k=1}^{N} \frac{f_{k+} - f_{k-}}{\omega_k} = \frac{1}{N}\sum_{k=1}^{N} \frac{1}{\omega_k}$$

$$= \frac{1}{N}\sum_{k=1}^{N} \frac{1}{2\sin\frac{k\pi}{2(N+1)}} \sim \frac{\ln N + 1}{\pi}. \tag{38}$$

In Fig. 1, the corresponding analytical expectations for the asymptotic distribution $f_{k\pm}$ are plotted as curves for reference. This well explains the observed energy concentration in the low-frequency positive modes.

V. INTRA- AND INTERBRANCH ENERGY TRANSPORTS

Due to the total angular momentum conservation, the intra- and interbranch energy transports may behave quite differently. For the intrabranch energy transport, all the existing rules for 1D lattices remain valid. The only difference is that the number of incoming phonons must equal the number of outgoing ones. For example, the scattering process of "three incoming phonons and one outgoing phonon" is strictly forbidden, no matter how strong the nonlinearity is. The Chirikov overlap criterion also applies. This will be discussed in detail in the next section. For the interbranch energy transport, there exist some nontrivial processes which are trivial in the 1D cases or the intrabranch cases. As an example, the process $k_1 + k_1 + k_2 \to k_1 + k_1 + k_2$ means nothing in a 1D case since the incoming and outgoing phonons are completely identical. For the interbranch transport in the quasi-2D lattice, however, the process

$$k_{1+} + k_{1-} + k_{2-} \to k_{1-} + k_{1-} + k_{2+} \tag{39}$$

is nontrivial. The net effect is that two phonons with opposite signs exchange their signs. Apparently, in such a process, the quasimomentum conservation

$$\sum_{\text{in}} k \overset{N}{=} \sum_{\text{out}} k \tag{40}$$

holds, and more importantly, since $\omega_{k+} = \omega_{k-} = \omega_k$, $\forall k$, the energy conservation

$$\sum_{\text{in}} \omega_k - \sum_{\text{out}} \omega_k = 0 \tag{41}$$

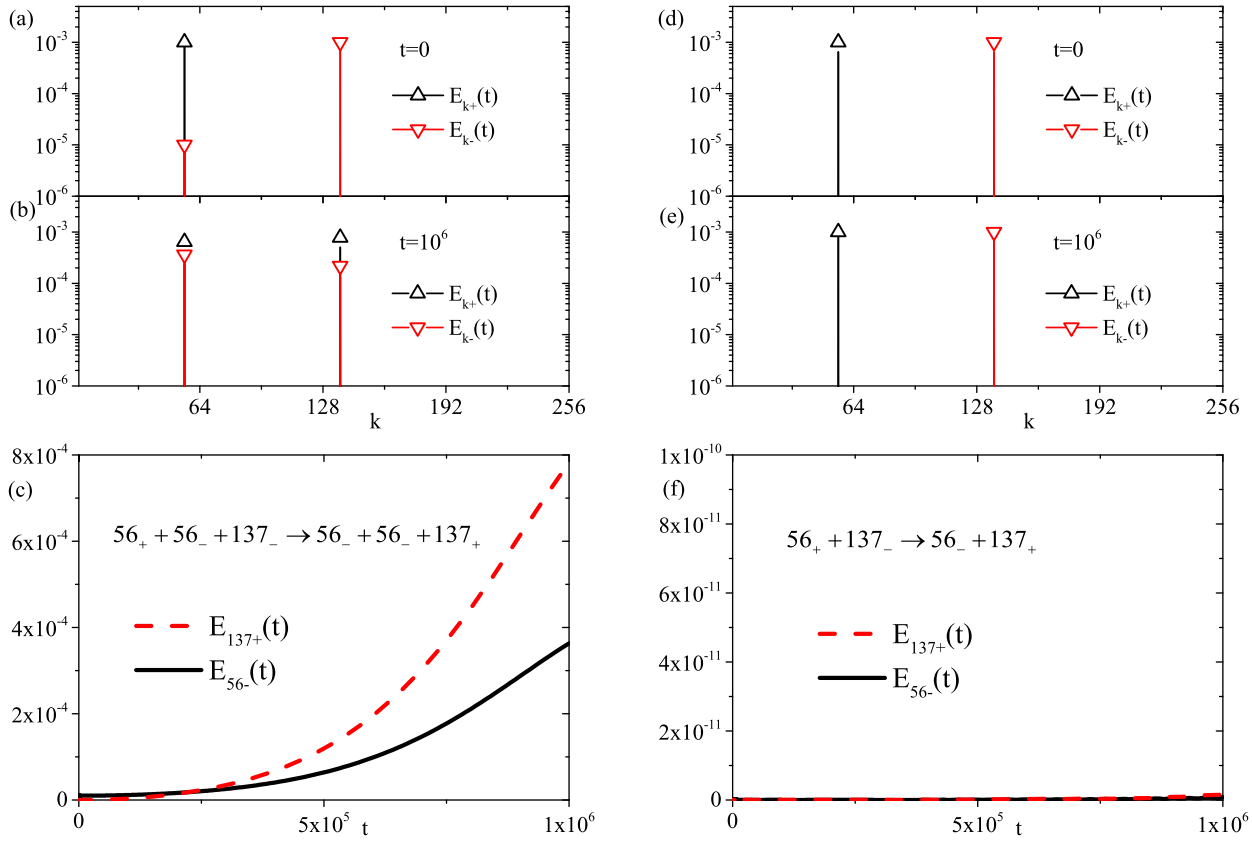

FIG. 2. Tests of the process described in Eq. (42) (left column) and its simplified version described in Eq. (43). Each average is taken over about 1000 independent realizations. [(a), (b)] The energy distributions for the former process at times $t = 0$ and 10^6, respectively. [(d), (e)] The energy distributions for the latter process at times $t = 0$ and 10^6, respectively. [(c), (f)] Mode energies E_{137+} and E_{56-} versus time t for the two processes.

is always satisfied exactly. Here the subscripts "in" and "out" denote the summations over the incoming and outgoing phonons, respectively; $\overset{N}{=}$ means equal modulus N [22,24]. Therefore, no nonlinearity-induced frequency broadening is required and thus the Chirikov criterion does not apply. Such interbranch scatterings are always possible, no matter how weak the nonlinearity is. However, given the facts that (1) during this type of process the angular momenta in the two branches are conserved separately, i.e., there is no interbranch angular momentum transport, and (2) the total mode energy of any k, i.e., $E_{k+} + E_{k-}$, is conserved, it is easily understood that the equipartition cannot be reached via these processes alone. They only provide some fast channels in the network involving all the normal modes. To form the whole network, the Chirikov-criterion-obeyed processes are still necessary.

Here we present an example for such a process. We simulate a lattice with $N = 256$, and choose $k_1 = 56$ and $k_2 = 137$; thus the process reads

$$56_+ + 56_- + 137_- \to 56_- + 56_- + 137_+. \tag{42}$$

Those two wave vectors can be chosen arbitrarily and the results will be basically the same. Initially, a quite low value of energy, 10^{-3}, is put into each of the modes 56_+ and 137_-, i.e., the 56th mode in the positive branch and the 137th mode in the negative branch. Besides, an even much lower energy, 10^{-5}, is put into mode 56_- as a seed. All other modes are empty [see Fig. 2(a)]. We observe the resulting energy distribution versus time t and find that the energy in the modes 56_- and 137_+ increases basically exponentially [see Fig. 2(c)]. As expected, due to the angular momentum conservation, $E_{56_-}/E_{137_+} = \omega_{56}/\omega_{137} \approx 0.4518$. At the time $t = 10^6$, the energy has largely moved from the modes 56_+ and 137_- to 56_- and 137_+ [see Fig. 2(b)]. This timescale is much shorter than the thermalization time $t_{\rm eq}$ for the average mode energy 10^{-3}. It is worth mentioning that the energy is shared only among the modes for $k = 56$ and 137. To move energy to other values of k, Chirikov-criterion-obeyed processes are necessary. However, the energy 10^{-3} is too low to meet the criterion.

Interestingly, the above-mentioned seed is necessary for the scattering; i.e., the simplified process

$$56_+ + 137_- \to 56_- + 137_+ \tag{43}$$

does not work. To confirm it, we remove the seed in mode 56_-; i.e., initially $E_{56_+} = E_{137_-} = 10^{-3}$ and all other modes are empty [see Fig. 2(d)]. The evolution of the system becomes quite different. We see that for the same long time, no change of the energy distribution can be detected [see Fig. 2(f)]. E_{56_-} and E_{137_+} remain zero [see Fig. 2(e)]. Note that the scale in the Y axis of Fig. 2(f) is more than five orders of magnitude lower than that of Fig. 2(c). Further studies are necessary to understand this finding.

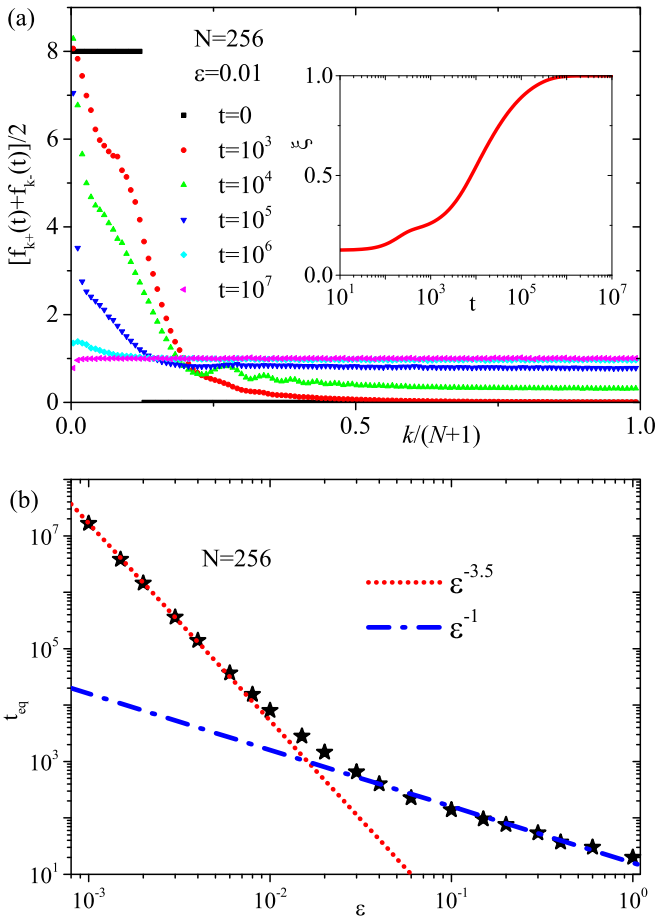

FIG. 3. (a) The rescaled mode energy distribution $f_{k\pm}$ for various times t. The energy is initially put into the lowest 1/8 frequency modes of both the two branches uniformly. The particle number $N = 256$, and the average mode energy $\varepsilon = 0.01$. Inset: The normalized quantity ξ versus time t. It approaches asymptotically the equipartition value 1. (b) The thermalization time $t_{\rm eq}$ versus ε. Each average is taken over more than 2000 independent realizations.

VI. THERMALIZATION PROCESS FROM ZERO ANGULAR MOMENTUM INITIAL CONDITIONS

Finally, we study the thermalization processes that end at true equipartition states. To guarantee it, the total angular momentum J of the initial states must be zero. The simplest choice might be that the initial energy is symmetrically shared by the positive and negative branches, i.e., $E_{k+} = E_{k-}$, $\forall k$ [40]. In such a case, due to the symmetry, $f_{k+}(t)$ and $f_{k-}(t)$ should be always statistically identical. Therefore, to reduce the fluctuation, we plot $[f_{k+}(t) + f_{k-}(t)]/2$. Since the inter-branch energy exchange is not displayed, we may concentrate on the intrabranch energy transport.

In Fig. 3, the rescaled mode energy distribution for various times t is plotted. The energy is initially put into the lowest 1/8 frequency modes of both the two branches. In contrast to the nonzero J cases, the equipartition process can be clearly observed. The distribution becomes more and more even and ξ approaches 1.

The thermalization time $t_{\rm eq}$ versus the average mode energy ε is plotted in Fig. 3(b). $t_{\rm eq}$ increases rapidly as energy density ε decreases. Like the case in the 1D FPU-β lattice [25], double scalings in the low- and high-ε limits are clearly observed. $t_{\rm eq} \sim \varepsilon^{-1}$ is observed in the high-ε limit. In the low-ε case, we expect that the power exponent would approach asymptotically -4, which has been observed in the 1D FPU-β lattice for the irreversible six-wave interactions [22,25,27]. However, a noticeable discrepancy appears. In a quite wide regime of ε, $t_{\rm eq}$ follows not ε^{-4} but $\varepsilon^{-3.5}$ very well. We naturally attribute it to the finite ε effect and expect that the power exponent would approach finally -4, but in an even much lower ε regime. Due to computational difficulties, we are not able to confirm it numerically.

The $t_{\rm eq} \sim \varepsilon^{-1}$ type of fast thermalization is possible if the Chirikov overlap criterion [34] is satisfied. The idea is that the phonon modes in a finite system are discrete and thus the left-hand side of Eq. (41) is commonly not exactly zero. However, the nonlinearity of the system broadens the mode frequencies. When such a broadening is large enough to cover the above-mentioned nonzero value, i.e.,

$$\sum_{\rm in} \tilde{\omega}_k - \sum_{\rm out} \tilde{\omega}_k \leqslant \Delta\omega, \tag{44}$$

fast thermalization happens [41,42]. Apparently, when the broadening is greater than the frequency distance between two adjacent modes, this condition will be easily satisfied. To study this, two factors need to be considered, i.e., the nonlinearity-induced frequency shift, which enlarges the frequency distance, and the nonlinearity-induced frequency broadening.

A. Nonlinearity-induced frequency shift

According to the effective phonon theory, the canonical normalized phonon modes are determined by the harmonic part of the Hamiltonian, and when a weak nonlinearity is applied, those modes remain but their frequencies are slightly enlarged. To determine those renormalized frequencies, a harmonic Hamiltonian with renormalization coefficient η is introduced to replace the original anharmonic Hamiltonian [8,12,43], i.e.,

$$H_R = \sum_{j=1}^{N} \frac{1}{2}|\vec{p}_j|^2 + \frac{\eta^2}{2}|\vec{q}_{j+1} - \vec{q}_j|^2. \tag{45}$$

The partition function for the renormalized lattice reads

$$Z_R = \int e^{-\frac{1}{T}H_R} d\vec{q} d\vec{p} = \left(\frac{2\pi T}{\eta}\right)^{2N}. \tag{46}$$

The Boltzmann constant k_B is set to unity here and after. The Helmholtz free energy reads

$$F_R = -T \ln Z_R = -2NT \ln \frac{2\pi T}{\eta}. \tag{47}$$

The free energy F of the anharmonic lattice satisfies

$$F \leqslant F_R + \langle H - H_R \rangle_R, \tag{48}$$

where $\langle\cdot\rangle_R$ denotes the ensemble average with respect to the canonical measure $e^{-\frac{1}{T}H_R}$.

$$\begin{aligned}\langle H - H_R\rangle_R &= \frac{\int\int (H-H_R)e^{-\frac{1}{T}H_R}d\vec{q}d\vec{p}}{Z_R} \\ &= \sum_{j=1}^{N}\frac{K-\eta^2}{2}\langle\Delta x_j^2+\Delta y_j^2\rangle_R + \frac{\lambda}{4}\langle\Delta x_j^4 \\ &\quad + 2\Delta x_j^2\Delta y_j^2+\Delta y_j^4\rangle_R \\ &= \frac{NT}{\eta^4}(-\eta^4+K\eta^2+2\lambda T). \end{aligned} \tag{49}$$

To find the value of η that minimizes the upper bound of F, i.e., the right-hand side of Eq. (49), let

$$\frac{\partial(F_R+\langle H-H_R\rangle_R)}{\partial\eta^2} = \frac{NT}{\eta^6}(\eta^4-K\eta^2-4\lambda T) = 0. \tag{50}$$

The physically relevant root reads

$$\eta = \sqrt{\frac{K+\sqrt{K^2+16\lambda T}}{2}}, \tag{51}$$

which is slightly larger than that of the corresponding 1D FPU-β lattice [8,12,44], $\eta_{1D} = \sqrt{\frac{K+\sqrt{K^2+12\lambda T}}{2}}$. Note that η is mode independent due to the Gibbs measure [24,45]; thus all the phonon frequencies are enlarged by the same factor η, i.e.,

$$\tilde{\omega}_k = \eta\omega_k. \tag{52}$$

The left-hand side of Eq. (44) and the frequency spacing will also be enlarged by the same coefficient η, which is ε independent and grows as $\varepsilon^{\frac{1}{4}}$ in the low- and high-ε limits, respectively. Therefore, in the low-ε cases the shift is negligible.

$\tilde{\omega}_k$ can be numerically determined by the location of the peak of $|\hat{a}_k(\omega)|^2$, where $\hat{a}_k(\omega)$ denotes the Fourier transform of the complex normal variable $a_k(t)$ that is defined in Eq. (17). In Fig. 4(a), $|\hat{a}_k(\omega)|^2$ for various average mode energies ε in an equilibrium state for $N = 256$ and $k = 256$ is plotted. Both the nonlinearity-induced shift and broadening can be observed clearly. $\tilde{\omega}_k$, i.e., where the peak of $|\hat{a}_k(\omega)|^2$ is located, versus ε is plotted in Fig. 4(b). The analytical expectation in Eq. (51) is also plotted as the curve. The agreement is quite good. Not surprisingly, like the cases in the 1D FPU-β lattice [8] and the 2D FPU-β scalar lattice [43], there exists a very slight overestimation.

B. Nonlinearity-induced frequency broadening

The nonlinearity-induced frequency broadening can also be measured by $\hat{a}_k(\omega)$. In the linear cases, $|\hat{a}_k(\omega)|^2$ takes the form of a δ function that is located at ω_k. When nonlinearity presents, the distribution diffuses. In order to quantitatively measure the degree of the broadening, we define the broadening width $\delta\omega_k$ of the mode k as the width of the central regime, the power in which equals half of the total value, i.e.,

$$\frac{\int_{\tilde{\omega}_k-\frac{\delta\omega_k}{2}}^{\tilde{\omega}_k+\frac{\delta\omega_k}{2}}|\hat{a}_k(\omega)|^2d\omega}{\int_0^\infty|\hat{a}_k(\omega)|^2d\omega} = \frac{1}{2}. \tag{53}$$

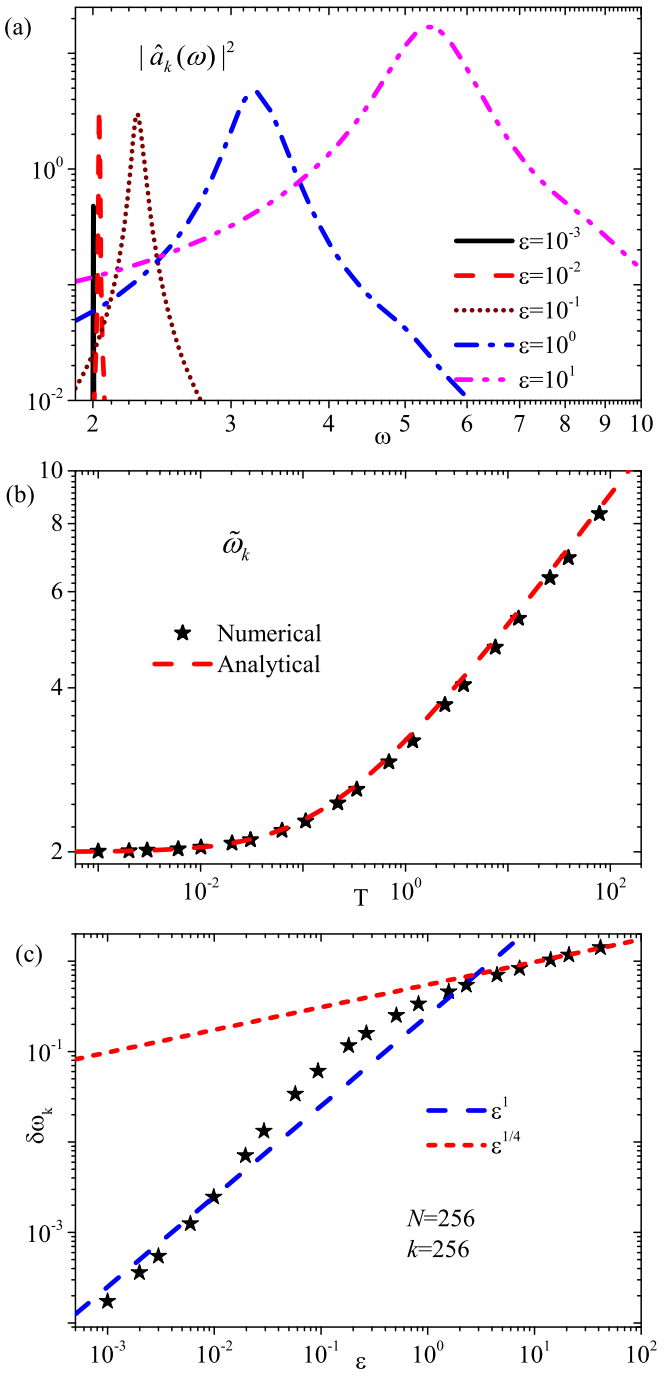

FIG. 4. (a) $|\hat{a}_k(\omega)|^2$ for various average mode energy ε. (b) $\tilde{\omega}_k$ versus ε. The symbols denote the locations of the peaks of $|\hat{a}_k(\omega)|^2$ in (a) and the curve denotes the analytical expectation in Eq. (52). (c) The broadening width $\delta\omega_k$ versus ε. $N = 256$ and $k = 256$. Each average is taken over about 1600 independent realizations.

In the cases of large fluctuations, this definition is much more robust in numerical calculation, compared with the standard deviation and the half-height width of $|\hat{a}_k(\omega)|^2$.

The frequency broadening $\delta\omega_k$ versus ε is plotted in Fig. 4(c). It is expected that in the low-energy ε cases, the broadening is proportional to ε [25], while in the large-ε limit, scaling analysis indicates a $\varepsilon^{\frac{1}{4}}$ growth for the potential of Eq. (2) having the highest order of r^4. The ε^1 and

$\varepsilon^{\frac{1}{4}}$ dependence in the small- and large-ε limits, respectively, are observed clearly. Since the shift and broadening are both basically system size N independent and the distance between adjacent modes is inversely proportional to the particle number N, it is easy to understand that the larger the system size the easier the Chirikov criterion is satisfied.

VII. SUMMARY

To summarize, we study the thermalization process in a 1D lattice with 2D motions. Unlike many other widely studied models, besides the total energy conservation, the total angular momentum J in this model is also conserved. Due to this conservation, a system from a nonzero-J initial state can never reach an equilibrium state, in which J must be zero. In such cases, energy concentration to a few low-frequency modes is observed. We suppose the asymptotic state maximizes the rescaled spectral entropy under the conditions of both the energy and angular momentum conservations; the counterintuitive distribution is then analytically explained.

The phonon modes in this lattice consist of two branches, positive and negative. Coincidentally, each phonon in the positive (negative) branch takes one unit of positive (negative) angular momentum, regardless of its wave vector k. As a consequence, the intra- and interbranch energy transports behave quite differently. The intrabranch energy transport obeys all the existing rules for phonon scattering in 1D lattices. The Chirikov overlap criterion still applies. However, any process with different numbers of incoming and outgoing phonons is strictly forbidden.

More importantly, as for the interbranch energy transport, there exist some nontrivial processes which are trivial in 1D lattices and intrabranch transport. In these processes, some phonons in the two branches exchange their signs and the quasimomentum and energy conservations are always satisfied exactly. Therefore, no nonlinearity-induced frequency broadening is required; this kind of processes are always possible no matter how weak the nonlinearity is. They provide some fast channels for energy exchange between the two branches. However, since these fast channels are not able to form a network involving all the normal modes, the overall thermalization process is still governed mainly by the Chirikov-criterion-obeyed scatterings. Consequently, like the cases in 1D lattices [25], double scaling of the equipartition time t_{eq} is still expected. This has been confirmed by our numerical simulations.

It is well known that the conserved quantities play a key role in energy transport. For example, heat conduction in 1D lattices with and without total momentum commonly behaves entirely differently [46]. The former one is generally anomalous, i.e., the heat conductivity diverges in the thermodynamic limit, whereas the latter one is commonly finite. It is naturally expected that the angular momentum conservation in this model may also play a crucial role in heat conduction and more in-depth studies are necessary to reveal it.

ACKNOWLEDGMENTS

This work was supported by the National Natural Science Foundation of China under Grant No. 12075316. Computational resources were provided by the Physical Laboratory of High Performance Computing at Renmin University of China.

[1] E. Ott, *Chaos in Dynamical Systems* (Cambridge University Press, Cambridge, UK, 1993).
[2] M. Hénon, Integrals of the Toda lattice, Phys. Rev. B **9**, 1921 (1974); H. Flaschka, The Toda lattice. II. Existence of integrals, *ibid.* **9**, 1924 (1974).
[3] E. Fermi, J. Pasta, and S. Ulam, in *Collected Papers* Vol. 2, edited by E. Fermi (University of Chicago Press, Chicago, 1965), p. 78.
[4] N. J. Zabusky and M. D. Kruskal, Interaction of "Solitons" in a Collisionless Plasma and the Recurrence of Initial States, Phys. Rev. Lett. **15**, 240 (1965).
[5] Y. Liu and D. He, Analytical approach to Lyapunov time: Universal scaling and thermalization, Phys. Rev. E **103**, L040203 (2021).
[6] N. Li, B. Li, and S. Flach, Energy Carriers in the Fermi-Pasta-Ulam β Lattice: Solitons or Phonons? Phys. Rev. Lett. **105**, 054102 (2010).
[7] N. Li, P. Tong, and B. Li, Effective phonons in anharmonic lattices: Anomalous vs. normal heat conduction, Europhys. Lett. **75**, 49 (2006).
[8] J. Liu, S. Liu, N. Li, B. Li, and C. Wu, Renormalized phonons in nonlinear lattices: A variational approach, Phys. Rev. E **91**, 042910 (2015).
[9] J. Liu, B. Li, and C. Wu, Variational approach to renormalized phonon in momentum-nonconserving nonlinear lattices, Europhys. Lett. **114**, 40002 (2016).
[10] N. Li, J. Liu, C. Wu, and B. Li, Temperature and frequency dependent mean free paths of renormalized phonons in nonlinear lattices, New J. Phys. **20**, 023006 (2018).
[11] N. Li and J. Liu, Accessing general relations for temperature coefficients of raman shifts in 2D materials, J. Phys.: Condens. Matter **32**, 285402 (2020).
[12] D. He, S. Buyukdagli, and B. Hu, Thermal conductivity of anharmonic lattices: Effective phonons and quantum corrections, Phys. Rev. E **78**, 061103 (2008).
[13] D. He, J. Thingna, J.-S. Wang, and B. Li, Quantum thermal transport through anharmonic systems: A self-consistent approach, Phys. Rev. B **94**, 155411 (2016).
[14] L. Xu and L. Wang, Dispersion and absorption in one-dimensional nonlinear lattices: A resonance phonon approach, Phys. Rev. E **94**, 030101(R) (2016).
[15] L. Xu and L. Wang, Resonance phonon approach to phonon relaxation time and mean free path in one-dimensional nonlinear lattices, Phys. Rev. E **95**, 042138 (2017).
[16] V. E. Zakharov, V. S. L'vov, and G. Falkovich, *Kolmogorov Spectra of Turbulence. 1. Wave Turbulence* (Springer, Berlin, 1992).
[17] V. Zakharov, F. Dias, and A. Pushkarev, One-dimensional wave turbulence, Phys. Rep. **398**, 1 (2004).
[18] A. J. Majda, D. W. McLaughlin, and E. G. Tabak, A one-dimensional model for dispersive wave turbulence, J. Nonlinear Sci. **7**, 9 (1997).

[19] V. Zakharov, P. Guyenne, A. Pushkarev, and F. Dias, Wave turbulence in one-dimensional models, Physica D **152-153**, 573 (2001), Advances in Nonlinear Mathematics and Science: A Special Issue to Honor Vladimir Zakharov.

[20] Y. V. Lvov and S. Nazarenko, Noisy spectra, long correlations, and intermittency in wave turbulence, Phys. Rev. E **69**, 066608 (2004).

[21] S. Chibbaro, G. Dematteis, C. Josserand, and L. Rondoni, Wave-turbulence theory of four-wave nonlinear interactions, Phys. Rev. E **96**, 021101(R) (2017).

[22] M. Onorato, L. Vozella, D. Proment, and Y. V. Lvov, Route to thermalization in the α-fermi-pasta-ulam system, Proc. Natl. Acad. Sci. USA **112**, 4208 (2015).

[23] S. W. Jiang, H. Lu, D. Zhou, and D. Cai, Stochastic linearization of turbulent dynamics of dispersive waves in equilibrium and non-equilibrium state, New J. Phys. **18**, 083028 (2016).

[24] B. Gershgorin, Y. V. Lvov, and D. Cai, Interactions of renormalized waves in thermalized Fermi-Pasta-Ulam chains, Phys. Rev. E **75**, 046603 (2007).

[25] Y. V. Lvov and M. Onorato, Double Scaling in the Relaxation Time in the β-Fermi-Pasta-Ulam-Tsingou Model, Phys. Rev. Lett. **120**, 144301 (2018).

[26] S. Lepri, Relaxation of classical many-body Hamiltonians in one dimension, Phys. Rev. E **58**, 7165 (1998).

[27] W. Fu, Y. Zhang, and H. Zhao, Universal scaling of the thermalization time in one-dimensional lattices, Phys. Rev. E **100**, 010101(R) (2019).

[28] Z. Wang, W. Fu, Y. Zhang, and H. Zhao, Wave-Turbulence Origin of the Instability of Anderson Localization against Many-Body Interactions, Phys. Rev. Lett. **124**, 186401 (2020).

[29] M. Gallone, M. Marian, A. Ponno, and S. Ruffo, Burgers Turbulence in the Fermi-Pasta-Ulam-Tsingou Chain, Phys. Rev. Lett. **129**, 114101 (2022).

[30] W. Fu, Y. Zhang, and H. Zhao, Universal law of thermalization for one-dimensional perturbed Toda lattices, New J. Phys. **21**, 043009 (2019).

[31] L. Pistone, M. Onorato, and S. Chibbaro, Thermalization in the discrete nonlinear Klein-Gordon chain in the wave-turbulence framework, Europhys. Lett. **121**, 44003 (2018).

[32] Y. V. Lvov and E. G. Tabak, Hamiltonian Formalism and the Garrett-Munk Spectrum of Internal Waves in the Ocean, Phys. Rev. Lett. **87**, 168501 (2001).

[33] F. De Vita, G. Dematteis, R. Mazzilli, D. Proment, Y. V. Lvov, and M. Onorato, Anomalous conduction in one-dimensional particle lattices: Wave-turbulence approach, Phys. Rev. E **106**, 034110 (2022).

[34] F. M. Izrailev and B. V. Chirikov, Statistical properties of a nonlinear string, Sov. Phys. Dokl. **11**, 30 (1966).

[35] Y. Sun and L. Wang, Correlation functions and their universal connection during an extremely slow equilibration process, Phys. Rev. E **105**, 054114 (2022).

[36] S. Tamaki, M. Sasada, and K. Saito, Heat Transport via Low-Dimensional Systems with Broken Time-Reversal Symmetry, Phys. Rev. Lett. **119**, 110602 (2017); D. Mao and L. Wang, Green-Kubo algorithm in the calculation of anomalous heat conduction for models with and without sound mode, Eur. Phys. J. B **93**, 39 (2020).

[37] R. Livi, M. Pettini, S. Ruffo, M. Sparpaglione, and A. Vulpiani, Equipartition threshold in nonlinear large Hamiltonian systems: The Fermi-Pasta-Ulam model, Phys. Rev. A **31**, 1039 (1985).

[38] C. Goedde, A. Lichtenberg, and M. Lieberman, Chaos and the approach to equilibrium in a discrete sine-Gordon equation, Physica D **59**, 200 (1992).

[39] G. Benettin and A. Ponno, Time-scales to equipartition in the Fermi-Pasta-Ulam problem: Finite-size effects and thermodynamic limit, J. Stat. Phys. **144**, 793 (2011).

[40] We have also tested other initial states with zero total angular momentum. The equipartition can always be reached.

[41] B. Callegari, M. C. Carotta, C. Ferrario, G. L. Vecchio, and L. Galgani, Stochasticity thresholds in the Fermi-Pasta-Ulam model, Nuov. Cim. B **54**, 463 (1979).

[42] L. Galgani and G. Lo Vecchio, Stochasticity thresholds for systems of coupled oscillators, Nuov. Cim. B **52**, 1 (1979).

[43] Y. Guo, Y. Sun, and L. Wang, Energy diffusion in two-dimensional momentum-conserving nonlinear lattices: Lévy walk and renormalized phonon, Phys. Rev. E **107**, 014109 (2023).

[44] T. Dauxois, M. Peyrard, and A. R. Bishop, Dynamics and thermodynamics of a nonlinear model for DNA denaturation, Phys. Rev. E **47**, 684 (1993).

[45] C. Alabiso, M. Casartelli, and P. Marenzoni, Nearly separable behavior of Fermi-Pasta-Ulam chains through the stochasticity threshold, J. Stat. Phys. **79**, 451 (1995).

[46] S. Lepri, R. Livi, and A. Politi, Thermal conduction in classical low-dimensional lattices, Phys. Rep. **377**, 1 (2003); A. Dhar, Heat transport in low-dimensional systems, Adv. Phys. **57**, 457 (2008); A. Dhar, A. Kundu, and A. Kundu, Anomalous heat transport in one dimensional systems: A description using non-local fractional-type diffusion equation, Front. Phys. **7**, 159 (2019); G. Benenti, S. Lepri, and R. Livi, Anomalous heat transport in classical many-body systems: Overview and perspectives, *ibid.* **8**, 292 (2020); G. Benenti, D. Donadio, S. Lepri, and R. Livi, Non-Fourier heat transport in nanosystems, Riv. Nuovo Cim. **46**, 105 (2023).